HHS Public Access

Author manuscript

Cancer J. Author manuscript; available in PMC 2016 May 01.

Published in final edited form as:

Cancer J. 2015 ; 21(3): 194–205. doi:10.1097/PPO.0000000000000117.

Optical Imaging, Photodynamic Therapy and Optically-Triggered Combination Treatments

Srivalleesha Mallidi, PhD[#], **Bryan Q. Spring, PhD**[#], and **Tayyaba Hasan, PhD**[*]

Wellman Center for Photomedicine, Massachusetts General Hospital, Boston, MA 02114

[#] These authors contributed equally to this work.

Abstract

Optical imaging is becoming increasingly promising for real-time image-guided resections and combined with photodynamic therapy (PDT), a photochemistry-based treatment modality, optical approaches can be intrinsically “theranostic”. Challenges in PDT include precise light delivery, dosimetry and photosensitizer tumor localization to establish tumor selectivity, and like all other modalities, incomplete treatment and subsequent activation of molecular escape pathways are often attributable to tumor heterogeneity. Key advances in molecular imaging, target-activatable photosensitizers and optically active nanoparticles that provide both cytotoxicity and a drug release mechanism, have opened exciting avenues to meet these challenges. The focus of the review is optical imaging in the context of PDT but the general principles presented are applicable to many of the conventional approaches to cancer management. We highlight the role of optical imaging in providing structural, functional and molecular information regarding photodynamic mechanisms of action, thereby advancing PDT and PDT-based combination therapies of cancer. These advances represent a PDT renaissance with increasing applications of clinical PDT as a frontline cancer therapy working in concert with fluorescence-guided surgery, chemotherapy and radiation.

Keywords

Photodynamic therapy; molecular imaging; optical imaging; image-guided therapy; dosimetry; photosensitizer; activatable probes; optical coherence tomography; fluorescence imaging; hyperspectral imaging and photoacoustic imaging

Introduction

It is well known that survival of aggressive cancers has improved only marginally (~15%) within the last 30 years.[1] For instance, the most recent cancer statistics indicate that the 5-year survival rate of pancreatic cancer is a meager 7%.[1] The minimal improvement in survival rate of cancer patients points to the critical need for new treatment modalities that can work in concert with surgery, radiation and chemotherapy—the mainstays of modern

[*]To whom correspondence should be addressed to: Tayyaba Hasan, PhD Professor of Dermatology Professor of Health Sciences and Technology (Harvard-MIT) Wellman Center for Photomedicine, Harvard Medical School Massachusetts General Hospital 40 Blossom Street, (Bartlett 314), Boston, MA 02114 Phone: 617-726-6996 FAX: 617-724-1345 thasan@mgh.harvard.edu.

oncology. Furthermore, it is now clear that cancer imaging can play a vital role in optimizing and enhancing the impact of cancer therapy. Taking advantage of the technical improvements in various imaging modalities over the years, imaging has taken a center stage in the quest for developing effective treatments. In this review, we discuss the utility of optical imaging techniques for development, design and monitoring of photodynamic therapy (PDT), a photochemistry based therapeutic modality, and novel PDT-based combination therapies. It is to be noted that a number of principles developed here for PDT will also be applicable to several other therapeutic modalities used in cancer.

PDT offers temporal and spatial control due to two components.[2] First, the photosensitizer (PS, a photoactivatable drug) is excited with light of a specific wavelength to react with its neighboring environment for generation of reactive oxygen species (Fig. 1). The PS can be specifically targeted to the tumor compartment utilizing various methodologies[3] such as immunoconjugates[4] or nanoconstructs.[5] Second, light delivery provides spatiotemporal control to cause regional tumor tissue damage while sparing surrounding healthy tissues – a critical need in treatment of tumors such as glioblastoma in the brain. The time between PS administration and light irradiation provides temporal control of the therapy while the specific location of light illumination provides spatial control. That is, PDT possesses an intrinsic dual selectivity for targeted lesions. Only where light and PS are present in adequate quantities will there be selective tissue damage. In addition, the PS used in PDT is inherently a theranostic agent; i.e., the molecule also has optical absorption and fluorescence emission properties. Hence, fluorescence imaging is generally employed to monitor PS uptake in the tumor and PS fluorescence holds promise for fluorescence-guided resection (FGR) as is approved in Europe for both brain[6] and bladder cancer.[7] Furthermore, the advantage of using the PS for FGR is that it will enable follow-up PDT to mop up the surgical bed of any residual disease that could cause recurrence.

Optical imaging has already played a vital role in PDT dosimetry.[2] Various metrics of PS fluorescence are utilized for PDT dose design.[8] For example, the amount of PS at the treatment site before PDT and quantitative monitoring of changes in PS fluorescence before and after PDT, due to PS photobleaching during its production of reactive oxygen species, has been shown to correlate with treatment response in clinical subjects.[9] As another example, Zhou et al. demonstrated that variation in treatment response is reduced when the PDT light dose is adjusted according to PS uptake in the tumors.[10] These studies show the importance of fluorescence imaging in PDT dosimetry; however, probing PS fluorescence alone is not representative of the complex PDT mechanisms of action and subsequent therapeutic effects induced by PDT. Towards the goal of understanding other structural and functional changes in tumors, new optical imaging techniques such as optical coherence tomography (OCT), spectroscopic optical techniques and photoacoustic imaging are being employed. We review the utility of these advanced optical imaging techniques for guiding PDT by monitoring: (1) structural and functional changes in tissue; (2) dynamic molecular responses to PDT to guide optimal inhibition of treatment escape pathways; (3) highly-selective FGR and PDT utilizing targeted and/or activatable probes in concert with molecular imaging; and, (4) multimodal image-guided PDT using novel nanoconstructs. Broadly, optical imaging could provide early detection, guided resection, therapy monitoring

and design of treatment regimens. Aspects of these applications with specific examples within PDT are presented here and can be adapted to an array of other therapeutics.

1. Monitoring tumor structural and functional changes due to PDT action

The common practice in preclinical cancer research is to measure changes in tumor volume as the major metric of treatment efficacy. With development of functional optical imaging modalities, non-invasive high–resolution measurements can be performed to extract parameters such as changes in tumor blood vessel density, blood oxygenation and biomarker status. These factors have been explored and evaluated as useful predictive reporters of PDT treatment efficacy.[8,11] In this section, we highlight various optical imaging techniques that can be applied to monitor these endogenous mechanisms of contrast to report on PDT dosimetry and efficacy.

Optical monitoring of changes in tumor structure and volume due to PDT—To appropriately design therapeutic dose and to deliver light to the tumor, the knowledge on anatomical location, volume and structure of the tumor is a prerequisite. Optical imaging techniques such as fluorescence and bioluminescence do not generally provide 3D tumor volume and depth information. However, with the advent of OCT (an optical analogue of ultrasound)[12] the detailed anatomical picture of the tumor at microscopic resolution has become available—at least up to a few millimeters of tissue depth.[12] OCT systems are attractive for imaging tumor response to PDT for several reasons. First, OCT systems typically utilize wavelengths of light ranging from 850 to 1350 nm, where absorption due to hemoglobin in blood is low and beyond the absorption of most PSs with insufficient energy for photodynamic action. Second, OCT systems use relatively low irradiances in the range of hundreds of microwatts. These characteristics of OCT make it a safe imaging technique compatible with PDT for visualizing tumor volume and microvascular networks before and after PDT without activating or photobleaching the PS.[12,13] Third, real-time, high speed OCT systems enable online monitoring of tumor structural changes during PDT, making it a viable candidate for clinical translation as is already becoming the case in cardiovascular applications.[14]

OCT based monitoring of PDT has been employed in preclinical and clinical settings as depicted in Fig. 2. OCT was used to monitor PDT response of 3D tumor models that recapitulate cell-cell and cell-matrix interactions of the tumor.[15,16] The capability of OCT to rapidly capture depth-resolved images of these 3D models at nodular, cellular and subcellular level overcomes the slow depth scanning of traditional optical microscopy. Time lapse OCT of these 3D tumor models provided valuable insight into the structural dynamics of the nodules following PDT; i.e., the nodules disintegrated into smaller highly scattering apoptotic cell clusters within the first 12 hours post PDT.[15,16]

OCT was first utilized to monitor superficial tumor models (Fig. 2); i.e., tumors that are readily accessible and require minimal probe development, such as skin and oral cancers. In a study by Hamdoon et al., OCT images of a squamous cell carcinoma obtained before treatment aided PDT design by mapping out the tumor extent and margins.[20] Tomographic images taken post-PDT for up to 6 months revealed complete response to PDT. In another

study by Themstrup et al, OCT correctly identified all of the partial responses to PDT (also confirmed by histology).[19] To overcome OCT's inability to image deep tumors, several needle based probes are being developed. Recently McLaughlin et al performed interstitial OCT via a needle probe to image deep tumors in the breast.[21] The side-facing needle probe comprises miniaturized focusing optics and rotating machinery to obtain 3D volumetric images - similar to the pull back method required for comprehensive volumetric imaging of lumens.[22] OCT has ability to delineate a clear tumor boundary from surrounding adipose tissue and microarchitectural features of the tumor such as stromal regions. Limitations of OCT reported in literature are poor contrast in post therapy images due to extensive inflammation and edema.[19] Despite these limitations, OCT can play a major role in efficiently discriminating between tumor and non-involved healthy tissue margins prior to PDT thereby reducing damage of neighboring vital tissues.

Optical monitoring of structural and functional changes in tumor vasculature due to PDT—Tumors often contain tortuous microvasculature that offers excellent structural contrast compared to normal healthy tissue. Several optical imaging techniques (such as: intravital microscopy,[23] doppler OCT,[24] photoacoustic imaging,[25] and laser speckle imaging[26]) have been utilized to monitor PDT induced changes in vascular structure and blood flow in animal models (Fig. 3). These studies showed that vessel occlusion and platelet formation occurred within few hours post therapy. Utilizing intravital microscopy, we deduced that in PDT with verteporfin (or benzoporphyrin derivative monoacid A, a PS approved by the US Food and Drug Administration) a 15 min drug light interval yielded more vascular damage than a 3 hour drug light interval when all the PS is cleared out of the vasculature.[27] Indeed these findings helped stimulate the development of combined vascular and cellular targeted PDT regimens in our group and in the study by Chen et al[28] we showed that more effective outcome is achieved when both these tumor compartments are damaged simultaneously than either compartment alone.

Blood vessels contain hemoglobin, a powerful optical absorber with characteristic wavelength dependent optical properties that enable imaging for another functional parameter - blood oxygen saturation (StO_2) – that is representative marker of tumor oxygen consumption. This functional parameter can be measured with spectroscopic optical techniques due to different optical properties of oxygenated and deoxygenated hemoglobin. Oxygen is consumed during PDT and at later time points no oxygen exchange between tumor tissue and blood happens due to subsequent vascular shutdown. We, and others, have shown the utility of imaging changes in StO_2 due to PDT as a therapeutic efficacy prediction parameter.[11,29] In particular, the seminal work by the Foster[30] and Henderson[31] groups elucidated the effect of fluence rate on therapeutic efficacy based on changes in blood oxygen saturation. Various spectroscopic techniques that monitor the StO_2 have been reported[29] such as the studies by Yu et al [32] and Sunar et al.[33] Many of these techniques are point detection systems or provide 2D surface-weighted images with low resolution. Recently we demonstrated the utility of 3D photoacoustic imaging (PAI) not only to monitor StO_2 but also to predict the likelihood of therapeutic efficacy.[11] PAI is a technique that involves generation of ultrasonic waves due to thermoelastic expansion of an absorber, such as blood vessels, upon absorption of nanosecond pulsed laser energy (Fig. 4). The

photoacoustic principles and generation of blood oxygen saturation maps have been reviewed extensively elsewhere.[34,35] In our study we demonstrated that StO_2 within the tumor volume decreased significantly post PDT; i.e., an approximate change of 85% or more in StO_2 within the first 24 h following PDT was observed in tumors that responded well to the treatment. In contrast, tumors that did not show a significant change in StO_2 values were predicted as non-responders. Based on these observations, we designed a "treatment prediction" algorithm where 3D ultrasound and photoacoustic StO_2 images were used to precisely map out the treated and non-treated regions and to identify volumes of the tumor that could seed tumor regrowth due to insufficient vascular damage. These results are encouraging as the non-treated regions could be identified within 24 h of PDT by imaging as compared to 10-30 days post treatment using palpation or tumor volume measurements. Given the advances in the availability of PAI in the clinical setting, these results encourage the development of PAI as an important modality for therapy monitoring, especially those treatment modalities involving a change in StO_2 (e.g., PDT, radiation, anti-angiogenic therapy).

2. Optical monitoring of dynamic molecular responses to PDT

Optical biopsy for early cancer detection is an emerging paradigm in oncology.[36-42] Beyond searching for early cancers, optical imaging is also being used to monitor dynamic molecular signaling pathways that promote treatment escape. For example, PDT successfully kills most tumor cells, but as for any therapy, there are survivors that up-regulate specific molecular responses to promote resistance to cell death and to provide growth and survival support to the remaining cells. A number of secreted proteins, cell-surface receptor tyrosine kinases (RTKs) and intracellular factors mediate these signaling cascades. Online molecular imaging provides an opportunity to capture these signaling dynamics to guide and optimize the use of molecular-targeted therapies to mop up these bursts in molecular signaling events. Here, we highlight a few molecular pathways that have been imaged online to understand molecular signaling induced by PDT and to enhance the outcome of PDT.

In an elegant study, Foster and colleagues applied green fluorescent protein (GFP) imaging to monitor the expression of heat shock proteins (HSPs) following subcurative PDT both in vitro and in an animal model.[43] HSPs chaperone protein folding and unfolding to modulate a number of intracellular signaling factors—some of which have been shown to be critical for resisting cell death following PDT.[44,45] In this investigation, the temporal dynamics of HSP activation was imaged within EMT6 mouse mammary carcinoma cells stably transfected with a plasmid containing GFP under the control of an HSP70 promoter sequence. PDT was carried out for a range of light doses following incubation of the cells with the PS mtetrahydroxyphenylchlorin (mTHPC, or Foscan). This imaging study found rapid induction of tumor cell HSP expression in vivo within 6 h of subcurative PDT, which may hold clinical relevance for designing low-dose PDT regimens to stimulate an antitumor immune response using HSP as a tumor antigen.[46]

A second example that demonstrates the potential of fluorescence molecular imaging to design interventions is the study by Chang et al, where transient, elevated vascular

endothelial growth factor (VEGF) expression levels were observed in subcutaneous tumors following subcurative PDT using longitudinal molecular imaging.[47] VEGF is a secreted cytokine growth factor that—along with its receptors (e.g., VEGFR2)—represents a key molecular target of several antiangiogenic agents in clinical use. VEGF is involved in tumor angiogenesis, re-growth and survival post-PDT.[48-53] Upon secretion, a substantial population of VEGF is sequestered by the extracellular matrix (via the heparin binding domain of many VEGF isoforms) and remains localized to the tumor until its release by enzymatic cleavage. Once VEGF mobilizes beyond the basement membrane and into the vasculature, it becomes available for a host of angiogenic activities and for interactions with tissues distal to the tumor site. The VEGF molecular imaging investigation used a small animal hyperspectral fluorescence imaging system and a fluorophore-antibody conjugate (bevacizumab-Alexa Fluor 680) to label VEGF in vivo (Fig. 5A). Prior to this VEGF imaging study in a prostate cancer model, a positron emission tomography study using an ovarian cancer model also showed early promise in in-vivo visualization of VEGF,[54] however it was unknown whether or not longitudinal imaging of secreted molecules could be performed quantitatively and accurately. A critical technological development that has enabled sensitive optical molecular imaging is hyperspectral fluorescence imaging. Conventional fluorescence intensity imaging through a band pass filter samples a small portion of the emission spectrum. Because biological tissues are complex and heterogeneous, the strength of the autofluorescence signal varies within the tissue making it difficult to quantify fluorophore concentrations using this method. On the contrary, in hyperspectral fluorescence imaging a fluorescence emission spectrum is collected for each pixel. The resulting image “cube” is analyzed pixel-by-pixel using linear spectral deconvolution (“spectral unmixing”) to break the spectrum up into its individual component spectra (Fig. 5A). This enables accurate quantification of the fluorescence signal from specific fluorescent contrast agents and separation of their emission from the tissue autofluorescence.[55,56]

In the hyperspectral fluorescence imaging study by Chang et al., quantification of spectrally unmixed VEGF images of subcutaneous tumors was compared to quantification of tumor VEGF levels using biochemical assays (enzyme-linked immunosorbent assay) performed on pulverized tumor tissues following the imaging sessions. These biochemical assays confirmed the accuracy of VEGF concentrations determined by spectral unmixing image analysis (Fig. 5BE). Longitudinal tumor VEGF imaging revealed a transient up-regulation in VEGF secretion (peaking at ~6 hours and sustained for several days) in subcutaneous pancreatic and prostate xenograft tumor models.[47] Making use of these observations of transient increases in tumor VEGF secretion, we also found preliminary evidence that timed delivery of bevacizumab, to address the transient increase in VEGF, mitigates metastasis following PDT of prostate cancer.[57] Bevacizumab delivered outside the time window of initial VEGF up-regulation was significantly less effective. This suggests that the dynamics of VEGF are germane to its role in recurrent cancer. These findings underscore the need to further visualize and understand the spatiotemporal dynamics of cytokine growth factors and their receptors to provide guidance for timing the delivery of neutralizing agents, which will lead to more appropriate dosimetry and help to characterize new drug delivery systems for

cytokine- and RTK-targeted therapy with controlled release profiles matched to critical periods of the molecular signaling dynamics.

3. Photosensitizer fluorescence-guided resection and high-fidelity detection, monitoring and photodestruction utilizing activatable probes and optical imaging

Fluorescence-guided resection (FGR) is approved and in practice for resecting brain and bladder cancers in Europe.[7,58] FGR is performed with systemic administration of the non-fluorescent pro-PS, 5-aminolevulinic acid, that leads to intracellular accumulation of fluorescent protoporphyrin IX (PpIX) in cancer cells. In a promising multicenter phase III clinical trial enabling intraoperative visualization and resection of brain tumors, the FGR approach doubled the frequency of complete resection of malignant gliomas with an enhancement in progression free survival (Fig. 6A).[59] Inspired by this small-molecule pro-drug approach, a molecular-targeted, activatable approach extends tumor visualization and damage to the microscale (Fig. 6B) using activatable antibody-PS conjugates (explained in more detail below). A similar approach has been tested in humans, using folate-fluorescein conjugates for molecular targeting and intraoperative molecular fluorescence imaging to help surgeons identify ovarian cancer metastases. This study found that the molecular imaging approach facilitated the identification of more tumor deposits by surgeons compared with conventional bright-field illumination.[60] This development may ultimately translate to resection via FGR for more radical cytoreductive surgery, leaving less disease behind.[61] This approach is being further developed where PSs are used both as fluorescence resection contrast agents and as therapy agents for PDT to mop up residual cancer cells and infiltrates in the tumor resection bed, which offers promise to help prevent disease recurrence. Early promising results combining FGR and PDT have been reported by Eljamel et al[6] in glioblastoma patients.

Even with fluorescence-guided surgery, small deposits of drug-resistant cancer cells frequently escape standard therapies and go undetected until the emergence of lethal recurrent disease. These residual tumor deposits limit our ability to cure many cancers and cannot be detected using standard clinical imaging modalities. For instance, ultrasound, positron emission tomography and magnetic resonance imaging all have poor sensitivity for sub-centimeter tumors.[63,64] A recent advance is to utilize tumor biochemistry for tumor-confined PS activation, which in turn enables both tumor-selective PS fluorescence imaging and PDT.[4,65] Further developing this approach, a recent study combined tumor-activation with targeting of cell surface molecules overexpressed by cancer cells—termed tumor-targeted activation—to selectively damage disseminated microscopic disease. This molecular-targeted activatable approach extends the fidelity to the microscale and enables imaging and selective destruction of disseminated, microscopic tumors[4]. This approach, “tumor-targeted, activatable photoimmunotherapy” (taPIT), builds on seminal reports of photoimmunotherapy (PIT)—a targeted form of PDT[66-72] using antibody-PS conjugates—as well as elegant, activatable fluorescent[73-77] and photodynamic probes.[65,78] The same study, developed *in vivo* monitoring of cancer micrometastases using the same activatable and near infrared (NIR) photocytotoxic immunoconjugate used for taPIT (Fig. 7).[4] To demonstrate this concept, a dual-function, activatable immunoconjugate that targets cancer cells overexpressing the epidermal growth factor receptor (EGFR) was synthesized to serve both

as an imaging probe and a combinational therapeutic agent. The PIC integrates photodynamic and anti-EGFR therapeutic agents, and the photodynamic and fluorescence components become de-quenched (activated) upon cellular internalization and processing. Because cancer cells overexpressing the target surface molecules take up the immunoconjugates more efficiently, this targeted activation occurs predominantly within tumors and enhances tumor selectivity—based on extensive imaging and phototoxicology studies comparing immunoconjugates with low- and high-quenching efficiencies[60]. The immunoconjugate binds micrometastases with 93% sensitivity and 93% specificity in vivo, enabling accurate recognition of tumors as small as 30 μm in a clinically-motivated mouse model of disseminated, micrometastatic ovarian cancer.[4,79] Fluorescence microendoscopy was applied to characterize immonconjugate pharmacokinetics and tumor-selectivity dynamics—to determine the optimal time points for micrometastasis imaging and taPIT—and to quantitatively monitor micrometastasis destruction during therapy.[4]

Furthermore, off-target toxicity was significantly reduced with enhanced tumor reductions using high-dose taPIT.[4] Using wide field PDT, taPIT was able to reduce off-target toxicities and enabled safe application of a 17- to 50-fold greater photodynamic dose (photodynamic agent dose × light dose) compared to conventional non-targeted, “always-on” PDT agents as well as to targeted, “always-on” PIT agents.[4] First, this represents a significant advance—the enhanced tumor selectivity overcomes bowel toxicity (as evidenced by biodistribution, dose escalation and histopathology studies[4]), which has been the dose-limiting factor and the major hurdle identified in PDT clinical studies of peritoneal metastases.[82,83] Second, a single cycle of taPIT plus chemotherapy resulted in a 97% reduction of micrometastatic burden in the mouse model of ovarian cancer, whereas a single cycle of chemotherapy alone resulted in only a 3% reduction. The relatively poor response to chemotherapy alone is likely due to intrinsic chemoresistance—the OVCAR5 cancer cells used in this model have seven-fold resistance to cisplatin relative to a platinum-sensitive cell line[84] and contain a subpopulation of stem-like cells that are stimulated by chemotherapy.[85] This “theranostic” approach may ultimately facilitate the clinical diagnosis and treatment of early recurrent, drug-resistant disease that is missed by standard clinical imaging modalities—whilst alleviating the need for precise light delivery in PDT, which should help clinicians use PDT more broadly in the clinic.

4. Multi-modality imaging guided PDT with novel nanoconstructs

Nanotechnology methods are being applied to engineer constructs that are cancer theranostic agents (i.e., both imaging and therapy agents) and these multifunctional drug delivery systems are being explored by several groups. The National Cancer Institute Alliance for Nanotechnology in Cancer was founded to harness the power of nanotechnology and to radically change the way we diagnose, treat and prevent cancer. In PDT, nanoparticles are utilized to specifically deliver PS to the site of interest. As already mentioned, many PSs are suitable as fluorescence imaging contrast agents and can be utilized to track the tumor accumulation of nanoconstructs encapsulating the PS. Reviews by us and others[5,86-88] showcase myriad types of multi-functional nanoparticles that take advantage of the leaky tumor vasculature to deliver a high payload of PS to the tumor compartment whilst significantly lowering systemic release of the PS. Furthermore, obtaining accurate

quantification of tissue PS levels is necessary for adjustment of light dose to reduce inter-subject variation and improve treatment consistency.[10] As fluorescence imaging is a surface weighted modality and does not provide comprehensive quantification of PS levels in the 3D tumor volume, PAI has been proposed as an alternative.[34] Due to its high optical absorption properties compared to endogenous chromophores in the body, PS are also good photoacoustic contrast agents.[89] Recently we demonstrated that PAI can map the heterogeneous accumulation of methylene blue (optical absorption peak around 670 nm) loaded liposomes in brain tumors to aid in personalized PDT dosimetry.[90] As active PDT agents, a concern is that PS could be photobleached during imaging procedures. To enhance PS contrast by several fold and to reduce the photobleaching effects, nanoagents comprising of imaging agents such as plasmonic gold nanoparticles in addition to PS are utilized. Recently, Yan et al. designed and tested a novel photo-theranostic platform based on sinoporphyrin sodium (DVDMS) PS-loaded PEGylated graphene oxide (GO-PEG-DVDMS) for enhanced fluorescence/photoacoustic (PA) dual-modal imaging and combined photodynamic therapy (due to the PS) and photothermal (due to the graphene oxide) therapy. While the GO-PEG carrier drastically improves the fluorescence of loaded DVDMS via intramolecular charge transfer. Concurrently, DVDMS significantly enhances the near-infrared (NIR) absorption of GO for improved PA imaging and photothermal therapy.[91] More complex nanosystems such as the upconversion nanoparticles[92-94] and theranostic multi-compartmental liposomes[5,95,96] (Fig. 8) and porphyrosomes[97,98] offer great promise and are currently being tested for efficacy and toxicity in *in vitro* and animal models. These theranostic nanoagents together with optical imaging techniques that can monitor the nanoagent accumulation in tumor, deduce nano-molecular interactions[99] and obtain changes in structural and functional properties of the tumor, have the potential to make personalized PDT a reality.

Conclusions and Perspective

In summary, this review highlights the essential role of optical imaging at every stage of PDT, from disease detection to treatment design and planning and recurrence prediction. The development of optical imaging techniques to probe functional and molecular information has aided in revealing insights into mechanisms of action of PDT at both the microscopic and macroscopic levels and in preclinical and laboratory settings. To make optical imaging techniques a routine in the clinical setting, technologies need to be developed to image tumors in hard to reach places such as the brain. There has been tremendous momentum amongst research groups to bring these optical techniques into clinical use – for example photoacoustic mamoscopes and endoscopes are being developed for monitoring breast and gastrointestinal tract cancers by several groups.[100] Along with progress in imaging techniques, it is important to understand PDT-related mechanisms and develop relevant algorithms, combination therapies and standardized procedures that will aid in personalizing treatment with individualized dosimetry. It might be speculated realistically that in the future a patient will be screened for vascular, biomarker and tumor structural properties and PDT dosimetry and combination therapies will be designed according to this information. Finally, due to space limitations, the focus of this article has been optical methods of imaging and treatment, however, the principles developed and discussed here

should be applicable to many therapeutic approaches and could be key to personalized treatments.

Acknowledgments

Sources of support:

This work was supported by NIH grants F32CA165881 (to Dr. Mallidi), 5P01CA084203, R01CA156177, R01CA158415, R01CA160998 (to Dr. Hasan) and funds from Canon USA Inc.

References

1. Siegel RL, Miller KD, Jemal A. Cancer statistics, 2015. CA: A Cancer Journal for Clinicians. 2015; 65(1):5–29. [PubMed: 25559415]
2. Celli JP, Spring BQ, Rizvi I, Evans CL, Samkoe KS, Verma S, et al. Imaging and Photodynamic Therapy: Mechanisms, Monitoring, and Optimization. Chem. Rev. 2010; 110(5):2795–838. PMCID: PMC2896821. [PubMed: 20353192]
3. Verma S, Watt GM, Mai Z, Hasan T. Strategies for enhanced photodynamic therapy effects. Photochem Photobiol. 2007; 83(5):996–1005. [PubMed: 17880492]
4. Spring BQ, Abu-Yousif AO, Palanisami A, Rizvi I, Zheng X, Mai Z, et al. Selective treatment and monitoring of disseminated cancer micrometastases in vivo using dual-function, activatable immunoconjugates. Proc Natl Acad Sci U S A. 2014; 111(10):E933–42. [PubMed: 24572574]
5. Huang H-C, Hasan T. The “Nano” World in Photodynamic Therapy. Austin Journal of Biomedical Engineering. 2014; 2(3):1–4.
6. Eljamel MS, Goodman C, Moseley H. ALA and Photofrin fluorescence-guided resection and repetitive PDT in glioblastoma multiforme: a single centre Phase III randomised controlled trial. Lasers Med Sci. 2008; 23(4):361–7. [PubMed: 17926079]
7. Mark JR, Gelpi-Hammerschmidt F, Trabulsi EJ, Gomella LG. Blue light cystoscopy for detection and treatment of non-muscle invasive bladder cancer. Can J Urol. 2012; 19(2):6227–31. [PubMed: 22512972]
8. Wilson BC, Patterson MS, Lilge L. Implicit and explicit dosimetry in photodynamic therapy: a New paradigm. Lasers Med Sci. 1997; 12(3):182–99. [PubMed: 20803326]
9. Mallidi S, Anbil S, Lee S, Manstein D, Elrington S, Kositratna G, et al. Photosensitizer fluorescence and singlet oxygen luminescence as dosimetric predictors of topical 5-aminolevulinic acid photodynamic therapy induced clinical erythema. J. Biomed. Opt. 2014; 19(2):028001. [PubMed: 24503639]
10. Zhou X, Pogue BW, Chen B, Demidenko E, Joshi R, Hoopes J, et al. Pretreatment photosensitizer dosimetry reduces variation in tumor response. Radiation Oncology Biology. 2006; 64(4):1211–20.
11. Mallidi S, Watanabe K, Timerman D, Schoenfeld D, Hasan T. Prediction of tumor recurrence and therapy monitoring using ultrasound-guided photoacoustic imaging. Theranostics. 2015; 5(3):289–301. [PubMed: 25553116]
12. Vakoc BJ, Fukumura D, Jain RK, Bouma BE. Cancer imaging by optical coherence tomography: preclinical progress and clinical potential. Nature Publishing Group. Nature Publishing Group. 2012; 12(5):363–8.
13. Vakoc BJ, Lanning RM, Tyrrell JA, Padera TP, Bartlett LA, Stylianopoulos T, et al. Three-dimensional microscopy of the tumor microenvironment in vivo using optical frequency domain imaging. Nat Med. 2009; 15(10):1219–23. [PubMed: 19749772]
14. Jang I-K, Bouma BE, Kang D-H, Park S-J, Park S-W, Seung K-B, et al. Visualization of coronary atherosclerotic plaques in patients using optical coherence tomography: comparison with intravascular ultrasound. J. Am. Coll. Cardiol. 2002; 39(4):604–9. [PubMed: 11849858]
15. Jung Y, Nichols AJ, Klein OJ, Roussakis E, Evans CL. Label-Free, Longitudinal Visualization of PDT Response In Vitrowith Optical Coherence Tomography. Isr. J. Chem. 2012; 52(8-9):728–44. PMCID: PMC3538822. [PubMed: 23316088]

16. Evans CL, Rizvi I, Hasan T, de Boer JF. In vitro ovarian tumor growth and treatment response dynamics visualized with time-lapse OCT imaging. Opt Express. May 25. 2009; 17(11):8892–906. PMCID: PMC2836890. [PubMed: 19466138]
17. Evans CL, Rizvi I, Celli J, Abu-Yousif A, de Boer J, Hasan T. Proceedings of SPIE. Optical Methods for Tumor Treatment and Detection: Mechanisms and Techniques in Photodynamic Therapy XIX. SPIE. :75510J–75510J–5.
18. Aalders MCG, Triesscheijn M, Ruevekamp M, de Bruin M, Baas P, Faber DJ, et al. Doppler optical coherence tomography to monitor the effect of photodynamic therapy on tissue morphology and perfusion. J. Biomed. Opt. 2006; 11(4):044011–1. [PubMed: 16965168]
19. Themstrup L, Banzhaf CA, Mogensen M, Jemec GBE. Optical coherence tomography imaging of non-melanoma skin cancer undergoing photodynamic therapy reveals subclinical residual lesions. Photodiagnosis and Photodynamic Therapy. 2014; 11(1):7–12. [PubMed: 24280439]
20. Hamdoon Z, Jerjes W, Upile T, Hopper C. Optical coherence tomography-guided photodynamic therapy for skin cancer: case study. Photodiagnosis and Photodynamic Therapy. 2011; 8(1):49–52. [PubMed: 21333934]
21. McLaughlin RA, Quirk BC, Curatolo A, Kirk RW, Scolaro L, Lorenser D, et al. Imaging of Breast Cancer With Optical Coherence Tomography Needle Probes: Feasibility and Initial Results. Selected Topics in Quantum Electronics, IEEE Journal of. IEEE. 2012; 18(3):1184–91.
22. Yun SH, Tearney GJ, Vakoc BJ, Shishkov M, Oh WY, Desjardins AE, et al. Comprehensive volumetric optical microscopy in vivo. Nat Med. 2006; 12(12):1429–33. [PubMed: 17115049]
23. Khurana M, Moriyama EH, Mariampillai A, Wilson BC. Intravital high-resolution optical imaging of individual vessel response to photodynamic treatment. J. Biomed. Opt. International Society for Optics and Photonics. 2008; 13(4):040502–040502–3.
24. Standish BA, Yang VXD, Munce NR, Song L-MWK, Gardiner G, Lin A, et al. Doppler optical coherence tomography monitoring of microvascular tissue response during photodynamic therapy in an animal model of Barrett's esophagus. Gastrointestinal Endoscopy. 2007; 66(2):326–33. [PubMed: 17643708]
25. Xiang L, Xing D, Gu H, Yang D, Yang S, Zeng L, et al. Real-time optoacoustic monitoring of vascular damage during photodynamic therapy treatment of tumor. J. Biomed. Opt. 2007; 12(1): 014001–1. [PubMed: 17343476]
26. Smith TK, Choi B, Ramirez San Juan JC, Nelson JS, Osann K, Kelly KM. Microvascular blood flow dynamics associated with photodynamic therapy, pulsed dye laser irradiation and combined regimens. Lasers Surg. Med. 2006; 38(5):532–9. [PubMed: 16615132]
27. Chen B, Pogue BW, Hoopes PJ, Hasan T. Combining vascular and cellular targeting regimens enhances the efficacy of photodynamic therapy. Radiation Oncology Biology. 2005; 61(4):1216–26.
28. Chen B, Pogue BW, Hoopes PJ. Vascular and cellular targeting for photodynamic therapy. Crit Rev Eukaryot Gene Expr. 2006; 16(4):279–306. [PubMed: 17206921]
29. Woodhams JH, MacRobert AJ, Bown SG. The role of oxygen monitoring during photodynamic therapy and its potential for treatment dosimetry. Photochem. Photobiol. Sci. 2007; 6(12):1246–56. [PubMed: 18046479]
30. Foster TH, Hartley DF, Nichols MG, Hilf R. Fluence rate effects in photodynamic therapy of multicell tumor spheroids. Cancer Res. 1993; 53(6):1249–54. [PubMed: 8443805]
31. Henderson BW, Busch TM, Snyder JW. Fluence rate as a modulator of PDT mechanisms. Lasers Surg. Med. 2006; 38(5):489–93. [PubMed: 16615136]
32. Yu G, Durduran T, Zhou C, Wang H-W, Putt ME, Saunders HM, et al. Noninvasive monitoring of murine tumor blood flow during and after photodynamic therapy provides early assessment of therapeutic efficacy. Clin. Cancer Res. 2005; 11(9):3543–52. [PubMed: 15867258]
33. Sunar U, Rohrbach D, Rigual N, Tracy E, Keymel K, Cooper MT, et al. Monitoring photobleaching and hemodynamic responses to HPPH-mediated photodynamic therapy of head and neck cancer: a case report. Opt Express. 2010; 18(14):14969. [PubMed: 20639983]
34. Mallidi S, Luke GP, Emelianov SY. Photoacoustic imaging in cancer detection, diagnosis, and treatment guidance. Trends in Biotechnology. 2011; 29(5):213–21. [PubMed: 21324541]

35. Xu M, Wang LV. Photoacoustic imaging in biomedicine. Review of Scientific Instruments. 2006; 77(4):041101.
36. Lüdicke F, Gabrecht T, Lange N, Wagnières G, Van den Bergh H, Berclaz L, et al. Photodynamic diagnosis of ovarian cancer using hexaminolaevulinate: a preclinical study. Br J Cancer. 2003; 88(11):1780–4. [PubMed: 12771995]
37. Yelin D, Rizvi I, White WM, Motz JT, Hasan T, Bouma BE, et al. Nature Publishing Group. Three-dimensional miniature endoscopy. Nature. 2006; 443(7113):765–5. [PubMed: 17051200]
38. Hsiung P-L, Hardy J, Friedland S, Soetikno R, Du CB, Wu AP, et al. Detection of colonic dysplasia in vivo using a targeted heptapeptide and confocal microendoscopy. Nat Med. 2008; 14(4):454–8. [PubMed: 18345013]
39. Williams RM, Flesken-Nikitin A, Ellenson LH, Connolly DC, Hamilton TC, Nikitin AY, et al. Strategies for high-resolution imaging of epithelial ovarian cancer by laparoscopic nonlinear microscopy. Transl Oncol. 2010; 3(3):181–94. [PubMed: 20563260]
40. Pierce MC, Guan Y, Quinn MK, Zhang X, Zhang W-H, Qiao Y-L, et al. A pilot study of low-cost, high-resolution microendoscopy as a tool for identifying women with cervical precancer. Cancer Prevention Research. 2012; 5(11):1273–9. [PubMed: 22926339]
41. Ford TN, Lim D, Mertz J. Fast optically sectioned fluorescence HiLo endomicroscopy. J. Biomed. Opt. International Society for Optics and Photonics. 2012; 17(2):021105–57.
42. Zavaleta CL, Garai E, Liu JTC, Sensarn S, Mandella MJ, Van De Sompel D, et al. A Raman-based endoscopic strategy for multiplexed molecular imaging. Proc Natl Acad Sci U S A. 2013; 110(25):E2288–97. [PubMed: 23703909]
43. Mitra S, Goren EM, Frelinger JG, Foster TH. Activation of heat shock protein 70 promoter with meso-tetrahydroxyphenyl chlorin photodynamic therapy reported by green fluorescent protein in vitro and in vivo. Photochem Photobiol. 2003; 78(6):615–22. [PubMed: 14743872]
44. Gomer CJ, Ryter SW, Ferrario A, Rucker N, Wong S, Fisher AM. Photodynamic therapy-mediated oxidative stress can induce expression of heat shock proteins. Cancer Res. 1996; 56(10):2355–60. [PubMed: 8625311]
45. Ferrario A, Rucker N, Wong S, Luna M, Gomer CJ. Survivin, a member of the inhibitor of apoptosis family, is induced by photodynamic therapy and is a target for improving treatment response. Cancer Res. 2007; 67(10):4989–95. [PubMed: 17510430]
46. Castano AP, Mroz P, Hamblin MR. Photodynamic therapy and anti-tumour immunity. Nat. Rev. Cancer. 2006; 6(7):535–45. [PubMed: 16794636]
47. Chang SK, Rizvi I, Solban N, Hasan T. In vivo Optical Molecular Imaging of Vascular Endothelial Growth Factor for Monitoring Cancer Treatment. Clin Cancer Res. 2008; 14(13):4146–53. [PubMed: 18593993]
48. Ferrario A, Tiehl von KF, Rucker N, Schwarz MA, Gill PS, Gomer CJ. Antiangiogenic treatment enhances photodynamic therapy responsiveness in a mouse mammary carcinoma. Cancer Res. 2000; 60(15):4066–9. [PubMed: 10945611]
49. Solban N, Selbo PK, Pål SK, Sinha AK, Alok SK, Chang SK, et al. Mechanistic investigation and implications of photodynamic therapy induction of vascular endothelial growth factor in prostate cancer. Cancer Res. 2006; 66(11):5633–40. [PubMed: 16740700]
50. Nowak-Sliwinska P, van Beijnum JR, van Berkel M, van den Bergh H, Griffioen AW. Vascular regrowth following photodynamic therapy in the chicken embryo chorioallantoic membrane. 2010; 13(4):281–92.
51. Weiss A, van Beijnum UR, Bonvin D, Jichlinski P, Dyson PJ, Griffioen AW, et al. Low-dose angiostatic tyrosine kinase inhibitors improve photodynamic therapy for cancer: lack of vascular normalization. J. Cell. Mol. Med. 2014; 18(3):480–91. [PubMed: 24450440]
52. Nowak-Sliwinska P, Weiss A, Beijnum JRV, Wong TJ, Ballini J-P, Lovisa B, et al. Angiostatic kinase inhibitors to sustain photodynamic angio-occlusion. Journal of Cellular and Molecular Medicine. 2012; 16(7):1553–62. [PubMed: 21880113]
53. Ferrara N, Hillan KJ, Novotny W. Bevacizumab (Avastin), a humanized anti-VEGF monoclonal antibody for cancer therapy. Biochemical and Biophysical Research Communications. 2005; 333(2):328–35. [PubMed: 15961063]

54. Nagengast WB, de Vries EG, Hospers GA, Mulder NH, de Jong JR, Hollema H, et al. In vivo VEGF imaging with radiolabeled bevacizumab in a human ovarian tumor xenograft. Journal of Nuclear Medicine. Society of Nuclear Medicine. 2007; 48(8):1313–9.
55. Zimmermann T, Rietdorf J, Pepperkok R. Spectral imaging and its applications in live cell microscopy. FEBS Lett. 2003; 546(1):87–92. [PubMed: 12829241]
56. Mansfield JR, Gossage KW, Hoyt CC, Levenson RM. Autofluorescence removal, multiplexing, and automated analysis methods for in-vivo fluorescence imaging. J. Biomed. Opt. 2005; 10(4): 41207–7. [PubMed: 16178631]
57. Kosharskyy B, Solban N, Chang SK, Rizvi I, Chang Y, Hasan T. A Mechanism-Based Combination Therapy Reduces Local Tumor Growth and Metastasis in an Orthotopic Model of Prostate Cancer. Cancer Res. 2006; 66(22):10953–8. [PubMed: 17108133]
58. Eljamel S. Photodynamic applications in brain tumors: A comprehensive review of the literature. Photodiagnosis and Photodynamic Therapy. 2010; 7(2):76–85. [PubMed: 20510302]
59. Stummer W, Pichlmeier U, Meinel T, Wiestler OD. Fluorescence-guided surgery with 5-aminolevulinic acid for resection of malignant glioma: a randomised controlled multicentre phase III trial. Lancet Oncol. 2006
60. van Dam GM, Themelis G, Crane LMA, Harlaar NJ, Pleijhuis RG, Kelder W, et al. Intraoperative tumor-specific fluorescence imaging in ovarian cancer by folate receptor-α targeting: first in-human results. Nat Med. 2011; 17(10):1315–9. [PubMed: 21926976]
61. Nguyen QT, Tsien RY. Fluorescence-guided surgery with live molecular navigation - a new cutting edge. Nat. Rev. Cancer. 2013; 13(9):653–62. [PubMed: 23924645]
62. Zimmermann A, Ritsch-Marte M, Kostron H. mTHPC-mediated photodynamic diagnosis of malignant brain tumors. Photochem Photobiol. 2001; 74(4):611–6. [PubMed: 11683042]
63. Gadducci A, Cosio S, Zola P, Landoni F, Maggino T, Sartori E. Surveillance procedures for patients treated for epithelial ovarian cancer: a review of the literature. Int J Gynecol Cancer. 2007; 17(1):21–31. [PubMed: 17291227]
64. soussan M, Guetz Des G, Barrau V, Aflalo-Hazan V, Pop G, Mehanna Z, et al. Comparison of FDG-PET/CT and MR with diffusion-weighted imaging for assessing peritoneal carcinomatosis from gastrointestinal malignancy. Eur Radiol. 2012; 22(7):1479–87. [PubMed: 22358428]
65. Lovell JF, Liu TWB, Chen J, Zheng G. Activatable Photosensitizers for Imaging and Therapy. Chem. Rev. 2010; 110(5):2839–57. [PubMed: 20104890]
66. Mew D, Wat CK, Towers GH, Levy JG. Photoimmunotherapy: treatment of animal tumors with tumor-specific monoclonal antibody-hematoporphyrin conjugates. J. Immunol. 1983; 130(3): 1473–7. [PubMed: 6185591]
67. Oseroff AR, Ohuoha DD, Hasan TT, Bommer JC, Yarmush ML. Antibody-targeted photolysis: selective photodestruction of human T-cell leukemia cells using monoclonal antibody-chlorin e6 conjugates. Proc Natl Acad Sci U S A. 1986; 83(22):8744–8. [PubMed: 2877461]
68. Goff BA, Bamberg M, Hasan T. Photoimmunotherapy of human ovarian carcinoma cells ex vivo. Cancer Res. American Association for Cancer Research. 1991; 51(18):4762–7.
69. Goff BA, Hermanto U, Rumbaugh J, Blake J, Bamberg M, Hasan T. Photoimmunotherapy and biodistribution with an OC125-chlorin immunoconjugate in an in vivo murine ovarian cancer model. Br J Cancer. 1994; 70(3):474–80. [PubMed: 8080733]
70. van Dongen GAMS, Visser GWM, Vrouenraets MB. Photosensitizer-antibody conjugates for detection and therapy of cancer. Adv Drug Deliv Rev. Jan 13; 2004 56(1):31–52. [PubMed: 14706444]
71. Molpus KL, Hamblin MR, Rizvi I, Hasan T. Intraperitoneal photoimmunotherapy of ovarian carcinoma xenografts in nude mice using charged photoimmunoconjugates. Gynecologic Oncology. 2000; 76(3):397–404. [PubMed: 10684717]
72. Mitsunaga M, Ogawa M, Kosaka N, Rosenblum LT, Choyke PL, Kobayashi H. Cancer cell-selective in vivo near infrared photoimmunotherapy targeting specific membrane molecules. Nat Med. Nature Publishing Group. Dec. 2011; 17(12):1685–91.
73. Weissleder R, Tung C-H, Mahmood U, Bogdanov A Jr. In vivo imaging of tumors with protease-activated near-infrared fluorescent probes. Nat Biotechnol. 1999; 17(4):375–8. [PubMed: 10207887]

74. Olson ES, Jiang T, Aguilera TA, Nguyen QT, Ellies LG, Scadeng M, et al. Activatable cell penetrating peptides linked to nanoparticles as dual probes for in vivo fluorescence and MR imaging of proteases. Proc Natl Acad Sci U S A. 2010; 107(9):4311–6. [PubMed: 20160077]

75. Urano Y, Asanuma D, Hama Y, Koyama Y, Barrett T, Kamiya M, et al. Selective molecular imaging of viable cancer cells with pH-activatable fluorescence probes. Nat Med. Jan. 2009; 15(1):104–9. [PubMed: 19029979]

76. Ogawa M, Regino CAS, Choyke P, Kobayashi H. In vivo target-specific activatable near-infrared optical labeling of humanized monoclonal antibodies. Mol Cancer Ther. American Association for Cancer Research. 2009; 8(1):232–9.

77. Lee H, Akers W, Bhushan K, Bloch S, Sudlow G, tang R, et al. Near-infrared pH-activatable fluorescent probes for imaging primary and metastatic breast tumors. Bioconjugate Chem. 2011; 22(4):777–84.

78. Zheng G, Chen J, Stefflova K, Jarvi M, Li H, Wilson BC. Photodynamic molecular beacon as an activatable photosensitizer based on protease-controlled singlet oxygen quenching and activation. Proc Natl Acad Sci U S A. 2007; 104(21):8989–94. [PubMed: 17502620]

79. Spring BQ, Palanisami A, Hasan T. Microscale receiver operating characteristic analysis of micrometastasis recognition using activatable fluorescent probes indicates leukocyte imaging as a critical factor to enhance accuracy. J. Biomed. Opt. International Society for Optics and Photonics. 2014; 19(6):066006–6.

80. Savellano MD, Hasan T. Photochemical targeting of epidermal growth factor receptor: a mechanistic study. Clin Cancer Res. 2005; 11(4):1658–68. [PubMed: 15746071]

81. Abu-Yousif AO, Moor ACE, Zheng X, Savellano MD, Yu W, Selbo PK, et al. Epidermal growth factor receptor-targeted photosensitizer selectively inhibits EGFR signaling and induces targeted phototoxicity in ovarian cancer cells. Cancer Lett. Elsevier Ireland Ltd. Aug 28. 2012; 321(2): 120–7.

82. Hahn SM, Fraker DL, Mick R, Metz J, Busch TM, Smith D, et al. A phase II trial of intraperitoneal photodynamic therapy for patients with peritoneal carcinomatosis and sarcomatosis. Clin Cancer Res. 2006; 12(8):2517–25. [PubMed: 16638861]

83. Cengel KA, Glatstein E, Hahn SM. Intraperitoneal photodynamic therapy. Cancer Treat. Res. 2007; 134:493–514. [PubMed: 17633077]

84. Roberts D, Schick J, Conway S, Biade S, Laub PB, Stevenson JP, et al. Identification of genes associated with platinum drug sensitivity and resistance in human ovarian cancer cells. Br J Cancer. 2005; 92(6):1149–58. [PubMed: 15726096]

85. Meirelles K, Benedict LA, Dombkowski D, Pepin D, Preffer FI, Teixeira J, et al. Human ovarian cancer stem/progenitor cells are stimulated by doxorubicin but inhibited by Mullerian inhibiting substance. Proc Natl Acad Sci U S A. Feb 14. 2012; 109(7):2358–63. PMCID: PMC3289387. [PubMed: 22308459]

86. Rai P, Mallidi S, Zheng X, Rahmanzadeh R, Mir Y, Elrington S, et al. Development and applications of photo-triggered theranostic agents. Adv Drug Deliv Rev. 2010; 62(11):1094–124. [PubMed: 20858520]

87. Chatterjee DK, Fong LS, Zhang Y. Nanoparticles in photodynamic therapy: an emerging paradigm. Adv Drug Deliv Rev. 2008; 60(15):1627–37. [PubMed: 18930086]

88. Bechet D, Couleaud P, Frochot C, Viriot M-L, Guillemin F, Barberi-Heyob M. Nanoparticles as vehicles for delivery of photodynamic therapy agents. Trends in Biotechnology. 2008; 26(11): 612–21. [PubMed: 18804298]

89. Ho CJH, Balasundaram G, Driessen W, McLaren R, Wong CL, Dinish US, et al. Multifunctional photosensitizer-based contrast agents for photoacoustic imaging. Sci. Rep. Jan 1. 2014; 4:5342–2. [PubMed: 24938638]

90. Mallidi, S.; Huang, H-C.; Liu, J.; Mai, Z.; Hasan, T. Towards image-guided photodynamic therapy of Glioblastoma.. In: Kessel, DH.; Hasan, T., editors. SPIE BiOS. SPIE; 2013. p. 85681C-85681C–7.

91. Yan X, Hu H, Lin J, Jin AJ, Niu G, Zhang S, et al. Optical and photoacoustic dual-modality imaging guided synergistic photodynamic/photothermal therapies. Nanoscale. 2014

92. Wang X, Liu K, Yang G, Cheng L, He L, Liu Y, et al. Near-infrared light triggered photodynamic therapy in combination with gene therapy using upconversion nanoparticles for effective cancer cell killing. Nanoscale. The Royal Society of Chemistry. 2014; 6(15):9198–205.

93. Idris NM, Gnanasammandhan MK, Zhang J, Ho PC, Mahendran R, Zhang Y. In vivo photodynamic therapy using upconversion nanoparticles as remote-controlled nanotransducers. Nat Med. Nature Publishing Group. 2012; 18(10):1580–5.

94. Fan W, Shen B, Bu W, Chen F, He Q, Zhao K, et al. A smart upconversion-based mesoporous silica nanotheranostic system for synergetic chemo-/radio-/photodynamic therapy and simultaneous MR/UCL imaging. Biomaterials. 2014; 35(32):8992–9002. [PubMed: 25103233]

95. Spring B, Mai Z, Rai P, Chang S, Hasan T. Theranostic Nanocells for Simultaneous Imaging and Photodynamic therapy of Pancreatic Cancer. Proc. of SPIE. SPIE. 2010:755104–11.

96. Zheng LZ, Rai P, Spring B, Mai Z, Evans C, Hasan T. Combination therapy targeting EGFR/MET crosstalk using nanotechnology improves photodynamic therapy treatment of pancreatic cancer. Mol Cancer Ther. American Association for Cancer Research. 2009; 8(12 Supplement):A127–7.

97. Lovell J, Jin CS, Huynh EE, Jin H, Kim C, Rubinstein J, et al. Porphysome nanovesicles generated by porphyrin bilayers for use as multimodal biophotonic contrast agents. Nat Mater. 2011; 10(4): 324–32. [PubMed: 21423187]

98. Carter KA, Shao S, Hoopes MI, Luo D, Ahsan B, Grigoryants VM, et al. Porphyrin-phospholipid liposomes permeabilized by near-infrared light. Nature Commun. 2014; 5:3546–6. [PubMed: 24699423]

99. Mallidi S, Kim S, Karpiouk A, Joshi PP, Sokolov K. Visualization of Molecular Composition and Functionality of Cancer Cells using Nanoparticle-augmented Ultrasound-guided Photoacoustics. Photoacoustics. 2015 Epub Ahead of Print.

100. Yoon T-J, Cho Y-S. Recent advances in photoacoustic endoscopy. World J Gastrointest Endosc. 2013; 5(11):534–9. [PubMed: 24255745]

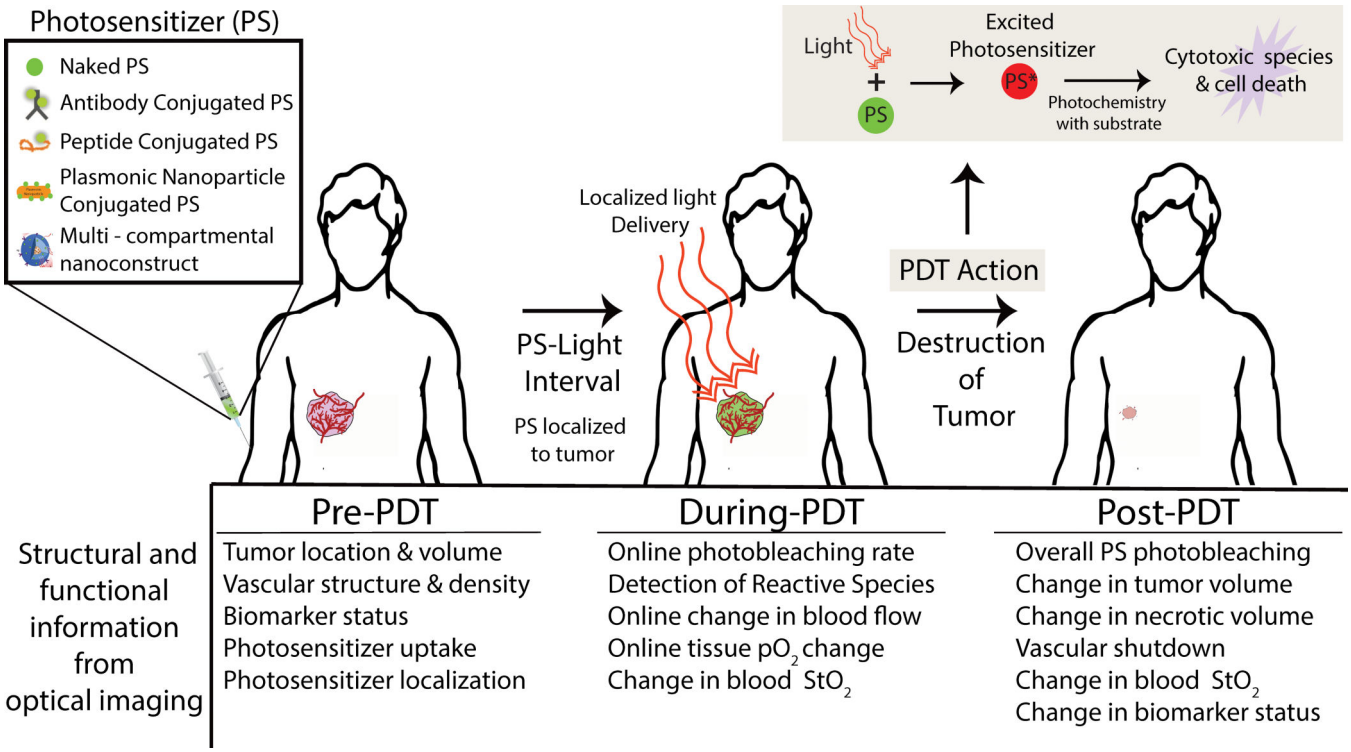

Figure 1.

General schematic representation of PDT procedure. The photosensitizer (PS) is a photoactivatable theranostic agent that upon light activation can serve as both an imaging agent and a therapeutic agent. The PS can be injected unconjugated or in various formulations to enhance specificity to the tumor (conjugated to an antibody or peptide, conjugated to plasmonic nanoparticles or encapsulated in multi-compartmental liposomes). After administration of the PS, light is locally delivered to the tumor after a given PS-light interval, i.e., at this time point, the PS has preferentially localized to the tumor. The localized light delivery adds a second layer of tumor selectivity even if the PS is present in non-tumor sites. The photochemistry resulting from the absorption of photon energy (photoexcitation) by the PS causes tumor destruction (upper right inset). Upon photoexcitation, the PS is promoted to an electronic excited state. The excited PS reacts with the surrounding environment (such as ground state molecular oxygen) to generate cytotoxic reactive species (such as singlet oxygen) leading to cell death. The bottom panel lists various structural and functional information that can be obtained using optical imaging techniques to guide PDT dosimetry; i.e., key parameters required for pretreatment planning, therapy monitoring and outcome assessment. StO_2 indicates blood oxygen saturation and pO_2 indicates oxygen partial pressure.

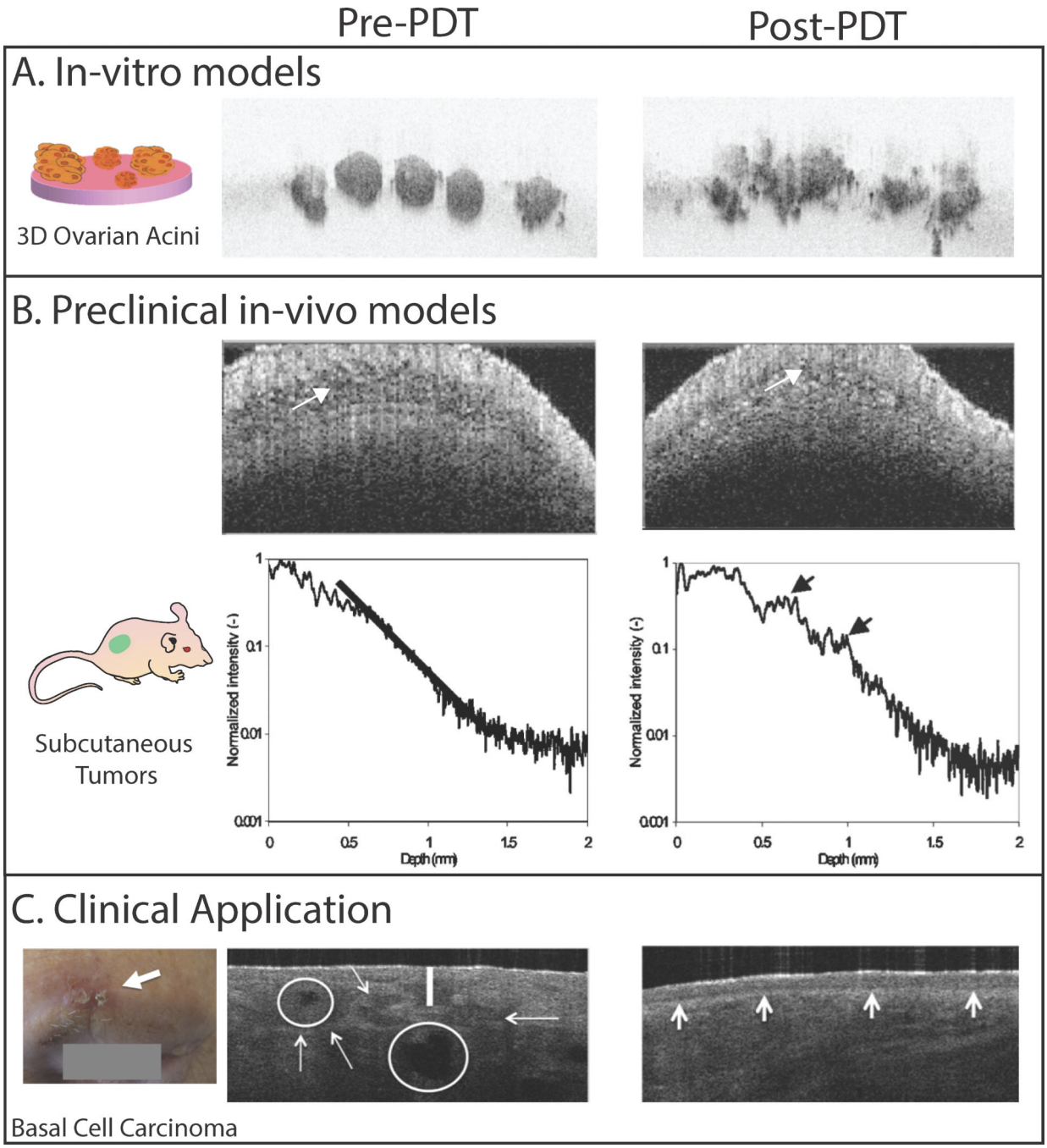

Figure 2.

Utility of OCT for visualizing PDT-induced structural changes in in-vitro 3D tumor nodules, preclinical animal models and human basal cell carcinoma in the clinic is shown here. **A.** Cross-sectional OCT image of 3D ovarian cancer acini are shown for time points before and 48 hours post PDT. Prior to PDT, the acini appear as small, solid and spherical structures. Due to PDT, a large-scale structural deformation in the acini can be observed.[17] The images measure 1.16 mm × 770 μm **B.** The OCT image (top row) and backscattering intensity profiles (bottom row) from a subcutaneous tumor before treatment and ~2 h after PDT are

shown here. In the pre- PDT image, the tumor has low backscattering intensity (white arrow). In the post-PDT image, the backscattering intensity increased due to PDT-induced tumor edema (white arrow) response in the tumor. The backscattering intensity profiles also show increased signal strength post-PDT (black arrows). Though differences between the pre and post-PDT tumor can be discerned in these images, it should be noted that increased signal levels at the surface could cause a decrease in the imaging penetration depth.[18] **C.** A clinical photograph of a superficial basal cell carcinoma located above the eyebrow (white arrow). The OCT image (3.5 mm × 2 mm) of the lesions shows the disruption of normal layering (white vertical line) and tumor location and size (white arrows). The tumors have a reflective core due to central necrosis (white circles). PDT was performed on this subject using methyl aminolevulinate as a pro-drug. OCT image at a 3-month follow-up post-PDT shows complete remission with a fully restore dermoepidermal junction in this subject. The images in panels A, B and C are adapted from Evans et al,[17] Aalders et al (2006)[18] and Themstrup et al (2014)[19] respectively.

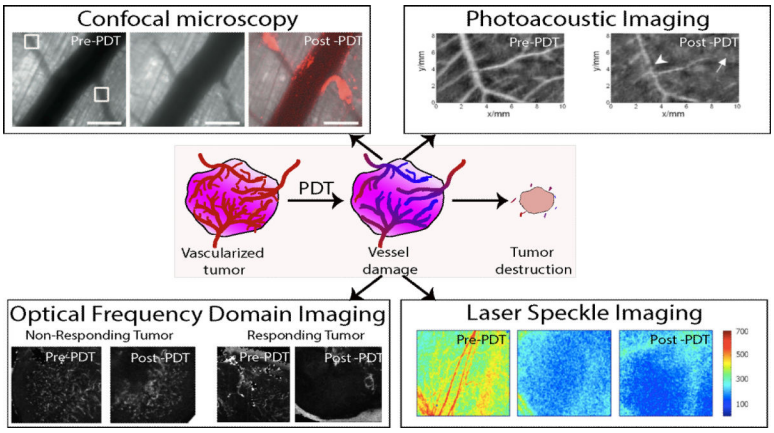

Figure 3.

Example images of various optical imaging techniques utilized for monitoring of vascular damage during PDT. **Confocal microscopy:** The images show vessels before, immediately after and 1.5 hours post-PDT. The white boxes in the pre-PDT image indicate the two regions receiving light irradiation 15 minutes post intravenous PS (verteporfin, or Visudyne 16 mg/kg dose) injection. The center image clearly shows vessel damage near the light irradiation spot. The third image showcases platelet (anti-CD41 antibody red fluorescence) formation in the vessels as a response to PDT. Scale bars are 200 μm in length.[23] **Photoacoustic imaging:** Vascular structures in a chicken chorioallantoic membrane (CAM) tumor model are obtained using photoacoustic imaging (also known as optoacoustic imaging). PDT was performed with the PS photoporphyrin IX disodium salt that was topically applied to the model. Post-PDT, vascular damage is seen in the vessels in the area of irradiation (white arrows). The study also showed no vessel damage during light-only treatment (images not shown).[25] **Optical frequency domain imaging:** OFDI is a second generation label free OCT based angiography technique, where the modulated optical scattering due to flowing blood can be detected and differentiated from static extra-vascular tissue. Here we show OFDI images from two tumors before and 4 days after PDT. Clearly in the tumor responding to the treatment, we observe complete damage of the vascular structure. There is not significant vessel damage in the non-responding tumor. This data suggests that monitoring of vasculature can serve as another biomarker to predict the treatment outcome early in the course of treatment. **Laser speckle imaging**: Representative laser speckle flow index images (5mm × 4 mm) of a rodent dorsal skin fold model are shown here. Images before intervention, immediately after and 18 hours after PDT are shown. PDT caused reduction in the speckle flow index due to vascular damage in the region.[26] The confocal microscopy, photoacoustic images and laser speckle images are obtained from Khurana et al (2008)[23], Xiang et al (2007)[25] and Smith et al (2006)[26] respectively. The OFDI images are unpublished data from our group.

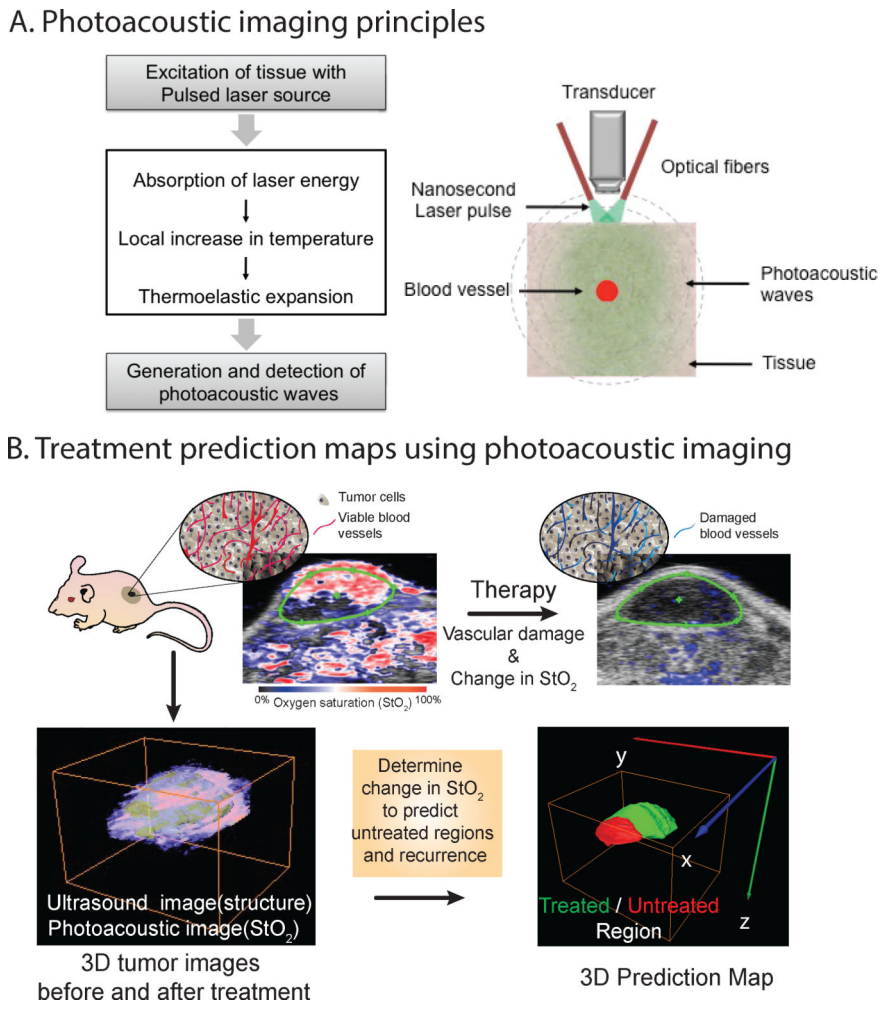

Figure 4.

A. Schematic diagram of photoacoustic signal generation is shown here. When a nanosecond laser pulse (satisfying the thermal-stress confinement conditions) irradiates a tissue optical absorber, such as a blood vessel, , photoacoustic signals are produced by the absorber due to thermoelastic expansion. An ultrasound transducer can be used to detect these photoacoustic signals that are digitally processed to form a photoacoustic image. The photoacoustic signal strength is proportional to the optical absorption properties of the absorber. Since oxygenated and deoxygenated hemoglobin have characteristic optical absorption properties, spectroscopic PAI can be used to detect the blood oxygenation saturation levels. **B.** A summary figure of our recent work[11] that demonstrates utility of photoacoustic imaging in treatment prediction is shown here. The top panel showcases schematic of tumor with blood vessels and related photoacoustic oxygen saturation maps of a subcutaneous tumor before and after PDT. The composite images have ultrasound image (grayscale image) in the background to identify the tumor region (green region of interest). The overlaid oxygen saturation map is pseudo-colored such that red represents highly oxygenated regions while blue represents hypoxic regions. The 2D images clearly show reduction in oxygen saturation post PDT (no red regions in the image). To further understand the nuances of treatment efficacy and to analyze which regions of tumor did not

receive the treatment, we performed 3D ultrasound and photoacoustic imaging of the tumors before and after PDT to produce a treatment prediction map. The red regions are the non-treated regions where the oxygen saturation has no decreased significantly post PDT while the green regions are the treated regions that showed more than 85% change in oxygen saturation values. Usually information on tumor regrowth post-therapy is available only after a detectable change in size is observed (10-30 days post-treatment in murine tumor models). Utilizing 3D PAI we were able to identify untreated regions and predict recurrence within 24 hours post-therapy. Images are adapted from Mallidi et al (2015).[11]

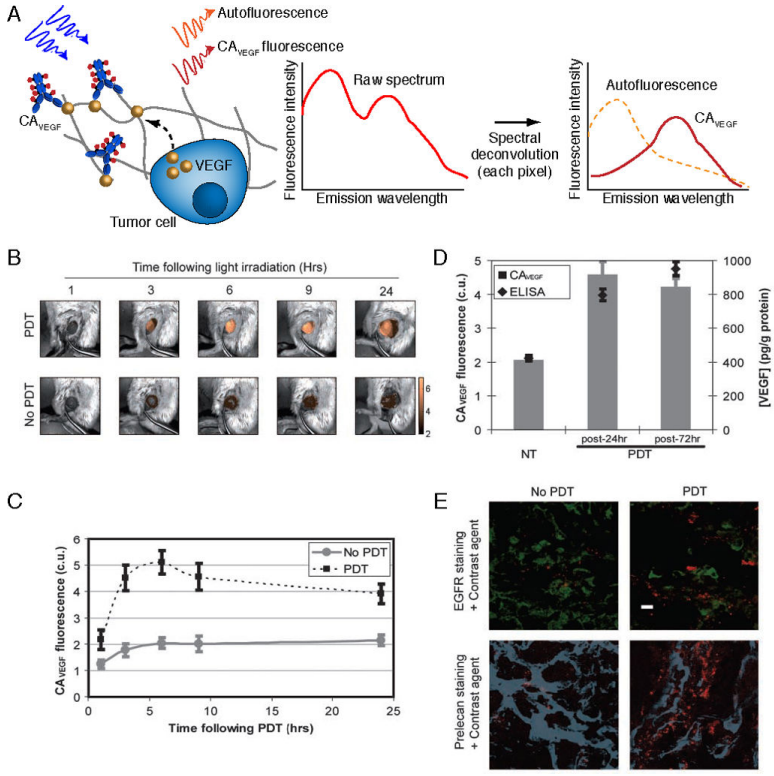

Figure 5.

In vivo molecular imaging of cytokine secretion dynamics in response to PDT. Here, fluorescence hyperspectral imaging has been applied to acquire a secreted VEGF level time course in subcutaneous prostate cancer tumors (PC-3 human prostate cancer cells) following PDT. **A**. Schematic of concepts for molecular imaging of secreted VEGF levels in tumors using fluorescence hyperspectral imaging to extract contrast agent signal from autofluorescence background. **B.** Overlay of Avastin-Alexa Flour 680 conjugate (false colored gold; contrast agent for secreted VEGF, CA_{VEGF}) fluorescence images (after spectral unmixing and calibration to a dye standard) and monochromatic reflectance images for a PDT-treated and an untreated control tumor. **C**. A time course of calibrated CA_{VEGF} intensities for PDT-treated versus untreated control tumors. The full time course reveals a peak in VEGF secretion within 6 to 24 h post-PDT that returns to its pre-PDT baseline value after 3–7 days. **D.** Validation of VEGF imaging using tumor VEGF protein concentrations measured by ELISA on whole tumor lysates. The gray columns indicate mean calibrated CA_{VEGF} intensity of untreated tumors (NT) and PDT-treated tumors at 24 h and 72 h following treatment; and, black diamonds indicate mean VEGF protein levels normalized by total protein concentration as determined by ELISA performed on whole tumor lysates. **E.** Localization of VEGF to cancer cells (green anti-EGFR stain) and heparin binding sites within the tumor ECM (blue, anti-perlecan stain) in ex vivo immunofluorescence images of cryosections from PDT-treated and untreated tumors. The mice were injected intravenously with CA_{VEGF} (red) and treated with PDT 24 h prior to tumor harvesting and cryosectioning. Scale bar, 10 μm. The transient peak in secreted VEGF levels represents an opportune and critical time period for inhibiting VEGF activity. Adapted from Chang et al (2008).[47]

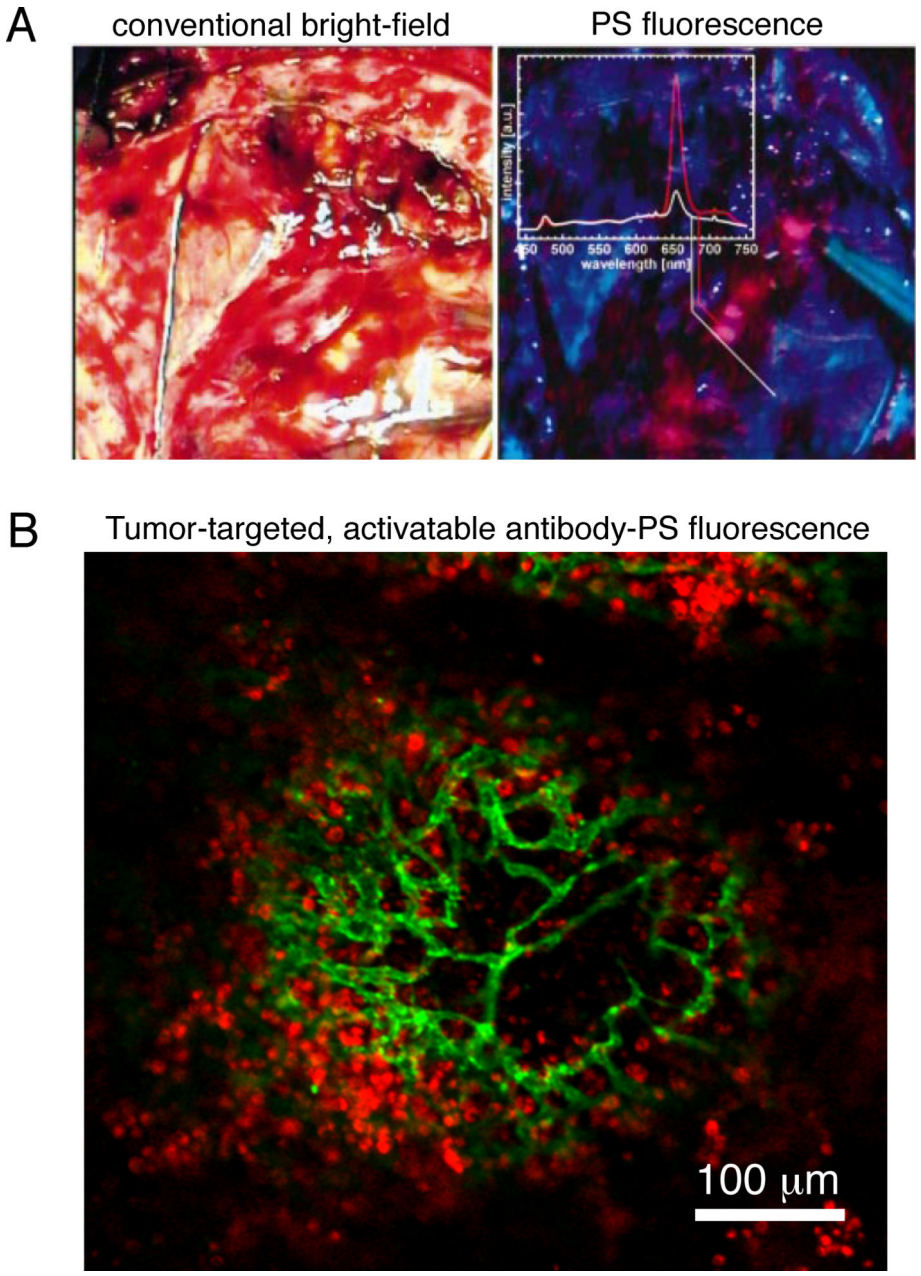

Figure 6.

A. Intraoperative images of a partially resected brain tumor comparing images obtained by conventional bright-field, or white light, imaging (left) versus PS (mTHPC) fluorescence imaging under blue light (A, right) The partially resected brain tumor is difficult to discern, while it is readily apparent in the PS fluorescence image of the same tissue. Image adapted from Zimmermann et al (2001).[62] **B.** *Ex vivo* tissue whole mount immunofluorescence image of a microscopic metastasis (micrometastasis) from a mouse model of peritoneal carcinomatosis where an EGFR-targeted, activatable PS-antibody conjugate (immunoconjugate) has been taken up and activated by tumor cells *in vivo* (red). An anti-mouse CD31 antibody has been applied to label endothelial cells (green). This development

is further explained in Figure 7 and enables tumor recognition and PDT with microscale selectivity. Image is adapted from Spring (2014) et al.[4]

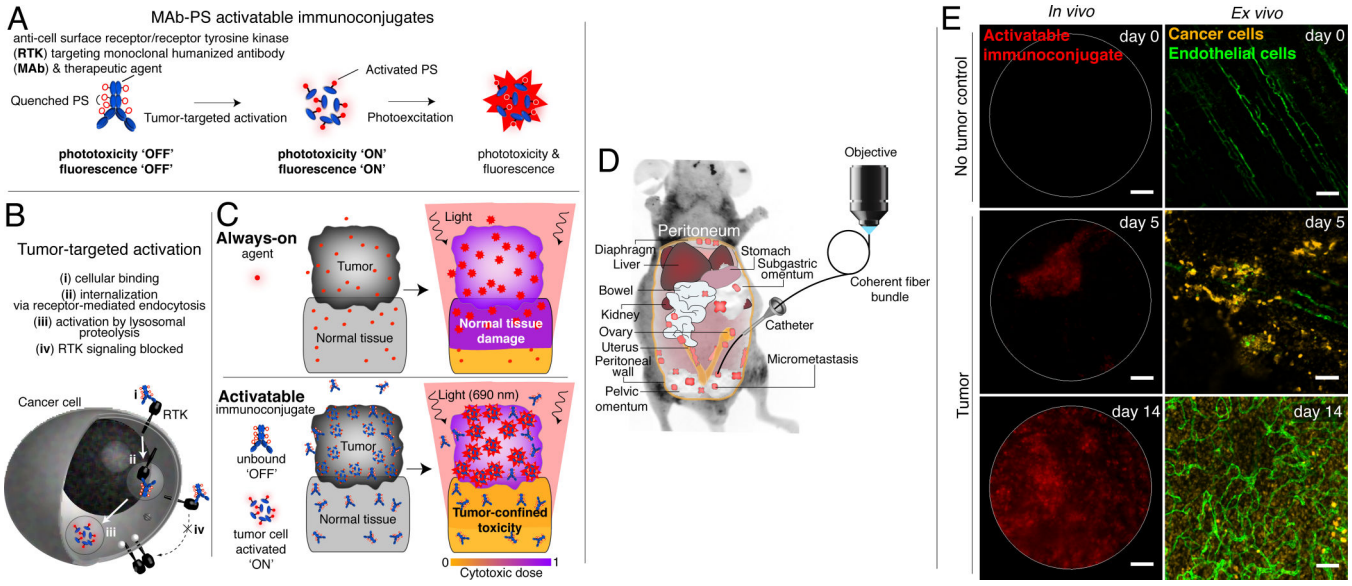

Figure 7.

Activatable immunoconjugates enable micrometastasis imaging and taPIT. **A.** Activatable immunoconjugates for taPIT are comprised of multiple self-quenching, photocytotoxic chromophores conjugated to antibodies that target and neutralize key molecules involved in tumorigenesis (e.g., EGFR). **B.** Cellular activation of the immunoconjugates via receptor-mediated endocytosis and lysosomal degradation. **C.** taPIT concept in which the immunoconjugate accumulates selectively within the tumor nodules, is activated by cellular processing,[80] inhibits molecular signaling[81] and imparts selective cytotoxicity to neoplasms upon irradiation.[4] **D.** To image disseminated peritoneal micrometastases in a mouse model of micrometastatic epithelial ovarian cancer, the microendoscope enters the body via a catheter traversing the abdominal wall. **E.** *In vivo* microendoscopy of activatable immunoconjugates (left) in control no-tumor and epithelial ovarian cancer mice (days 5 and 14 post-tumor inoculation). *Ex vivo* images (right) where an anti-human cytokeratin antibody has been applied to visualize the human epithelial cancer cells. An anti-mouse CD31 antibody labels the endothelial cells. Scale bars, 100 μm. Adapted from Spring et al (2014).[4]

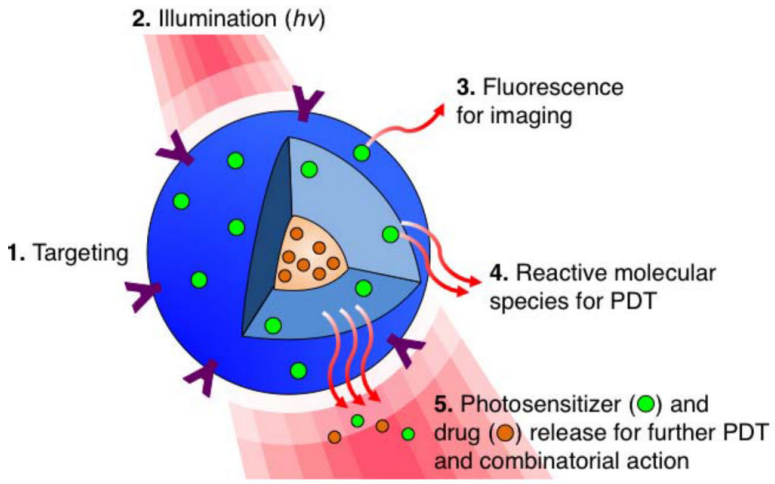

Figure 8.

Targeted, multi-compartment nanoconstructs co-deliver photosensitizers, molecular-targeted drugs and/or chemotherapeutics to the cell. (1) Surface modifications such as conjugating targeting moieties can be implemented to improve the tumor selectively of the nanoparticle. (2) Upon photoactivation, the (3) fluorescence signal generated from the excited PS can be used for imaging. (4) Light activation of the PS also results in reactive molecular species production for PDT, and (5) facilitates PS and drug release to facilitate interactive combination therapies with spatiotemporal control. Adapted from Huang et al (2014).[5]